

The monophenylhydrosilasesquioxanes $\text{PhH}_{n-1}\text{Si}_n\text{O}_{1.5n}$ where $n = 8$ or 10

Gion Calzaferri,^{*a} Claudia Marcolli,^a Roman Imhof^a and Karl W. Törnroos^{*b}

^a Institute of Inorganic and Physical Chemistry, University of Berne, Freiestrasse 3, 3000 Berne 9, Switzerland

^b Structural Chemistry, Stockholm University, S-106 91 Stockholm, Sweden

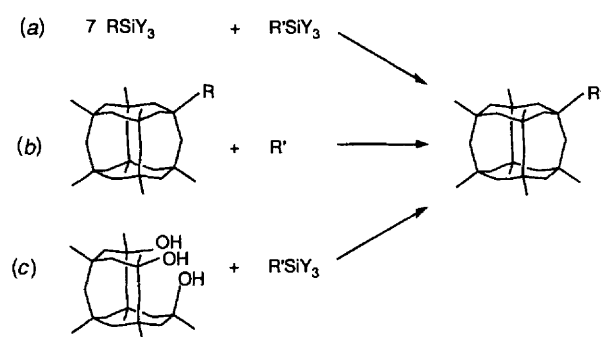
The first monosubstituted decasilasesquioxane, $\text{PhH}_9\text{Si}_{10}\text{O}_{15}$, and the analogous $\text{PhH}_7\text{Si}_8\text{O}_{12}$ molecule have been prepared and characterized by IR and Raman spectroscopy and X-ray crystallography. Both have crystallographic C_1 symmetry, but their cages exhibit an approximate C_s , and an effective C_3 , symmetry, respectively in the crystalline state. The IR and Raman spectra of the two molecules are very similar and reflect the close similarity observed for the spectra of $\text{H}_8\text{Si}_8\text{O}_{12}$ and $\text{H}_{10}\text{Si}_{10}\text{O}_{15}$. They have been treated as a superposition of the spectra of the siloxane cage $\text{H}_{n-1}\text{Si}_n\text{O}_{1.5n}$, $n = 8$ or 10 , the phenyl substituent and the connecting moiety $\text{O}_3\text{Si}-\text{C}(\text{CH})_2$ and assigned on the basis of spectral correlation and normal coordinate analysis. The siloxane cage vibrations are best understood by correlation with those of the unsubstituted cages, indicating that distortions of the Si_8O_{12} and $\text{Si}_{10}\text{O}_{15}$ cages caused by the substituent are small. A comparison of the Si-C stretching force constants indicates that Si-C_{vinyl} and Si-C_{phenyl} are of similar strength while the Si-C_{alkyl} bond is weaker. The notion of ring-opening vibrations, introduced for $(\text{HSiO}_{1.5})_{2n}$, $n = 2, 3, 4$, etc., is also applicable to $\text{PhH}_7\text{Si}_8\text{O}_{12}$ and $\text{PhH}_9\text{Si}_{10}\text{O}_{15}$. The phenyl substituent does not influence the frequency range of four- and five-membered ring-opening vibrations, however the number of such vibrations is increased.

The first spherosiloxane molecules of the general formula $(\text{RSiO}_{1.5})_{2n}$, $n = 2, 3, 4 \dots$, etc., can be traced back to studies published about 50 years ago.¹⁻⁴ For many years little attention was paid to this class of molecules, but in recent years an interesting chemistry has rapidly developed.⁵ A few monosubstituted heptahydrosilasesquioxanes $\text{RH}_7\text{Si}_8\text{O}_{12}$ with Si-CH₂-CHR', Si-CH=CHR', and Si-Co(CO)₄ bonds have been prepared and the crystal structures of $[\text{Co}(\text{CO})_4(\text{H}_7\text{Si}_8\text{O}_{12})]$ and $(\text{C}_6\text{H}_{13})\text{H}_7\text{Si}_8\text{O}_{12}$ have been determined.⁵⁻⁷ We now report the syntheses and crystal structures of the first monosubstituted decasilasesquioxane, $\text{PhH}_9\text{Si}_{10}\text{O}_{15}$ **2** and of $\text{PhH}_7\text{Si}_8\text{O}_{12}$ **1**, the first monosubstituted octasilasesquioxane with a Si-Ph bond. The vibrational structure of these molecules has been studied by IR and Raman spectroscopy. Normal coordinate analysis was carried out for unambiguous assignment of the fundamentals. We have analysed to what extent the vibrational spectra of **1** and **2** can be described as a superposition of the spectral features of the cages $\text{H}_8\text{Si}_8\text{O}_{12}$ and $\text{H}_{10}\text{Si}_{10}\text{O}_{15}$, respectively, and of the phenyl substituent. A preliminary analysis of this type was reported by us for $\text{RH}_7\text{Si}_8\text{O}_{12}$, $\text{R} = \text{CH}_2\text{CH}_2\text{Ph}$ or $\text{CH}=\text{CHPh}$.⁸ The Si-C stretching and the O-Si-C bending modes and the corresponding force constants are discussed in detail. The notion of ring-opening vibrations⁹ was introduced recently. They are normal modes of spherosiloxanes in which all Si-O stretching and/or O-Si-O angle-bending displacements of the considered ring are in phase. Monosubstitution of a hydrospherosiloxane causes a symmetry reduction. We discuss if and to what extent the notion of such vibrations remains applicable in this case.

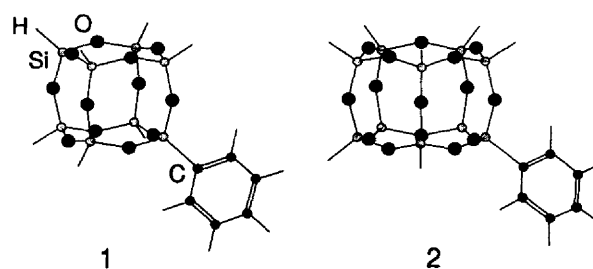
Results and Discussion

Synthesis

Three general ways for synthesizing monosubstituted $\text{R}'\text{R}''\text{Si}_n\text{O}_{1.5n}$ molecules have been used so far. They are summarized in Scheme 1. The classical route to spherosiloxanes (a) is polycondensation of trifunctional RSiY_3 monomers. We have applied it for the synthesis of the monophenylsilasesquioxanes $\text{PhH}_{n-1}\text{Si}_n\text{O}_{1.5n}$ ($n = 8$ or 10) which cannot be prepared



Scheme 1 Three general ways for synthesizing monosubstituted $\text{R}'\text{R}''\text{Si}_n\text{O}_{1.5n}$ molecules



by hydrosilation. Route (b) is probably the most generally applicable due to the easy availability of $\text{H}_8\text{Si}_8\text{O}_{12}$ and $\text{H}_{10}\text{Si}_{10}\text{O}_{15}$ ¹⁰ and most of the known mono- and di-substituted $\text{R}'\text{R}''\text{Si}_8\text{O}_{12}$ and $\text{R}'\text{R}''\text{Si}_6\text{O}_{9}$ molecules have been prepared this way.⁵ It can also be applied to other hydrosilasesquioxanes such as $\text{H}_{12}\text{Si}_{12}\text{O}_{18}$. Routes (a) and (b) lead to mixtures which can be separated, e.g. by HPLC, whereas (c), developed by Feher and co-workers^{11,12} has the advantage of giving one product only.

Molecular structure

We have reported earlier the structures of $\text{H}_8\text{Si}_8\text{O}_{12}$,¹³ $[\text{Co}(\text{CO})_4(\text{H}_7\text{Si}_8\text{O}_{12})]$,⁶ $(\text{C}_6\text{H}_{13})\text{H}_7\text{Si}_8\text{O}_{12}$,⁷ $\text{Cl}_8\text{Si}_8\text{O}_{12}$ ¹⁴ and

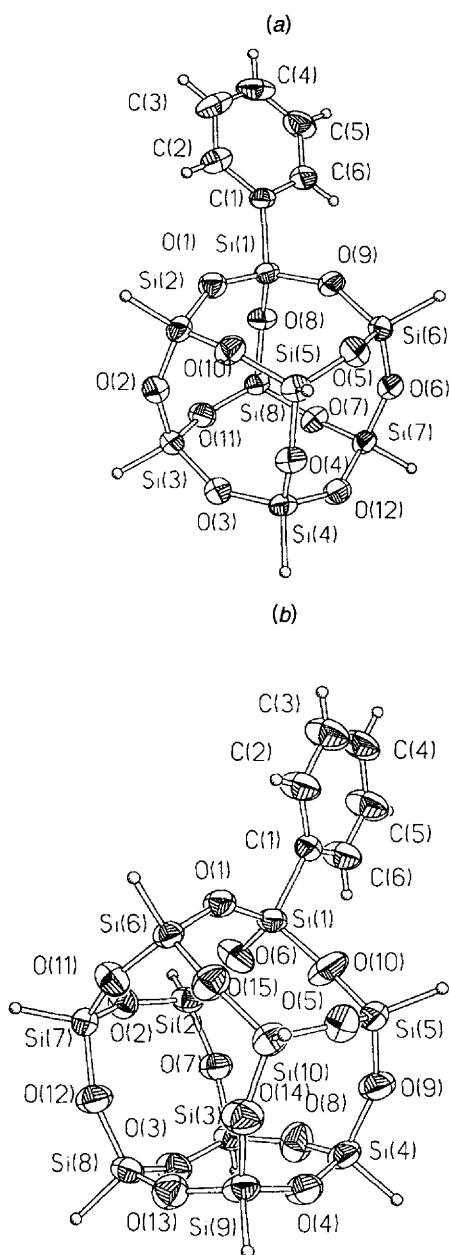


Fig. 1 Crystal structures of $\text{PhH}_7\text{Si}_8\text{O}_{12}$ (a) and $\text{PhH}_9\text{Si}_{10}\text{O}_{15}$ (b), with atomic labelling and anisotropic displacement parameters at the 30% probability level

$\text{H}_{10}\text{Si}_{10}\text{O}_{15}$.¹⁵ In the case of the octanuclear cages we have devoted our attention to the varying degree of lowering of the cage symmetry, $O_h \rightarrow T_h \rightarrow C_{3v} \rightarrow C_3$, occurring in these structures. Our measures have been the non-bonding body diagonal Si...Si distances and O(1,5) distances between opposite O atoms on the faces of the Si_8 cube, combined with the deviation of the two O atoms from each of the six body-diagonal planes on which they are ideally supposed to sit. The principal geometry parameters of compound **1** [Fig. 1(a), Table 1], are summed up by the following mean values: Si–O 1.612(5) Å; O–Si–O 109.3(5), Si–O–Si 148.4(2.2)°. The body diagonal Si...Si distances range from 5.353 to 5.397(1) Å, the difference being 0.044 Å. The maximum difference in O(1,5) distances between opposite O atoms is 0.294(3) Å with a mean of 0.171(87) Å. Finally, the average absolute departure of the O atoms out of the six body-diagonal planes (defined by the four Si atoms), being zero in O_h symmetry, is 0.050(24) Å while the mean departure is $-0.004(57)$ Å {all numbers in parentheses above and below represent the standard deviation s of the population

Table 1 Selected bond lengths (Å) and angles (°) for compound **1**

Si(1)–O(1)	1.614(2)	Si(5)–O(10)	1.601(2)
Si(1)–O(9)	1.618(2)	Si(5)–O(5)	1.610(2)
Si(1)–O(8)	1.623(2)	Si(5)–O(4)	1.614(2)
Si(1)–C(1)	1.834(3)	Si(6)–O(9)	1.607(2)
Si(2)–O(1)	1.601(2)	Si(6)–O(6)	1.616(2)
Si(2)–O(2)	1.604(2)	Si(6)–O(5)	1.616(2)
Si(2)–O(10)	1.617(2)	Si(7)–O(12)	1.607(2)
Si(3)–O(11)	1.613(2)	Si(7)–O(6)	1.608(2)
Si(3)–O(3)	1.615(2)	Si(7)–O(7)	1.611(2)
Si(3)–O(2)	1.619(2)	Si(8)–O(7)	1.607(2)
Si(4)–O(3)	1.613(2)	Si(8)–O(11)	1.611(2)
Si(4)–O(4)	1.615(2)	Si(8)–O(8)	1.613(2)
Si(4)–O(12)	1.616(2)		
O(1)–Si(1)–O(9)	109.11(11)	O(6)–Si(6)–O(5)	109.21(12)
O(1)–Si(1)–O(8)	109.10(12)	O(12)–Si(7)–O(6)	109.52(12)
O(9)–Si(1)–O(8)	107.95(11)	O(12)–Si(7)–O(7)	109.89(12)
O(1)–Si(1)–C(1)	109.46(13)	O(6)–Si(7)–O(7)	109.01(11)
O(9)–Si(1)–C(1)	109.94(12)	O(7)–Si(8)–O(11)	108.34(12)
O(8)–Si(1)–C(1)	111.23(12)	O(7)–Si(8)–O(8)	109.94(12)
O(1)–Si(2)–O(2)	109.37(13)	O(11)–Si(8)–O(8)	109.82(12)
O(1)–Si(2)–O(10)	109.64(12)	Si(2)–O(1)–Si(1)	149.18(14)
O(2)–Si(2)–O(10)	109.41(12)	Si(2)–O(2)–Si(3)	147.6(2)
O(11)–Si(3)–O(3)	109.84(12)	Si(4)–O(3)–Si(3)	149.49(14)
O(11)–Si(3)–O(2)	109.34(12)	Si(5)–O(4)–Si(4)	150.0(2)
O(3)–Si(3)–O(2)	108.84(13)	Si(5)–O(5)–Si(6)	145.4(2)
O(3)–Si(4)–O(4)	110.02(12)	Si(7)–O(6)–Si(6)	150.40(14)
O(3)–Si(4)–O(12)	108.87(12)	Si(8)–O(7)–Si(7)	150.99(14)
O(4)–Si(4)–O(12)	109.84(12)	Si(8)–O(8)–Si(1)	146.69(14)
O(10)–Si(5)–O(5)	109.06(12)	Si(6)–O(9)–Si(1)	150.67(14)
O(10)–Si(5)–O(4)	109.17(12)	Si(5)–O(10)–Si(2)	149.3(2)
O(5)–Si(5)–O(4)	110.11(12)	Si(8)–O(11)–Si(3)	147.6(2)
O(9)–Si(6)–O(6)	109.61(11)	Si(7)–O(12)–Si(4)	144.08(13)
O(9)–Si(6)–O(5)	109.21(12)		

where $s = \left[\frac{\sum_{i=1}^n (x_i - \bar{x})^2}{(n-1)} \right]^{1/2}$. The above numbers lead us to conclude that this structure essentially coincides with those reported earlier and that it retains an effective cage symmetry of C_3 .

Structure **2** [Fig. 1(b), Table 2], which consists of two ten-membered and five eight-membered rings, has an ideal cage symmetry of D_{5h} , but a crystallographic one of C_1 . It may, however, be considered as holding an approximate C_s symmetry. We have earlier reported an extensive analysis of the cage deformations of $\text{H}_{10}\text{Si}_{10}\text{O}_{15}$ (crystallographic symmetry C_2) and $\text{Me}_{10}\text{Si}_{10}\text{O}_{15}$,¹⁵ and so limit ourselves to reporting the average values for **2**, as they are generally in accordance with the foregoing decanuclear structures. The mean values are as follows: Si–O 1.602(12), 1.597(11) Å to bridging O atoms [O(1)–O(5)] and 1.612(6) Å in the ten-membered rings; O–Si–O 109.8(6), Si–O–Si 153.1(4.8), 148.2(2.8) over the bridging O atoms and 155.5(3.5)° in the ten-membered rings. The maximum O(1,5) distance difference between opposite O atoms in eight-membered rings is 0.223(5) Å [0.194(4) Å in $\text{H}_{10}\text{Si}_{10}\text{O}_{15}$] with a mean of 0.162(39) Å [0.153(79) Å in $\text{H}_{10}\text{Si}_{10}\text{O}_{15}$]. The corresponding mean O(1,5) distance in the ten-membered rings is 4.210(163) Å, ranging from 3.981(7) to 4.380(5) Å [4.118–4.343(5) Å in $\text{H}_{10}\text{Si}_{10}\text{O}_{15}$], illustrating a somewhat larger cage deformation and symmetry reduction from D_{5h} than in the case of $\text{H}_{10}\text{Si}_{10}\text{O}_{15}$ at 295 K. In all, the Si–O distance vs. Si–O–Si angle (α) comply well with the relationship for the spherosiloxanes¹⁵ $d(\text{Si}-\text{O}) = 1.59 + (180 - \alpha)^4 (2.1 \times 10^{-8})$, for both **1** and **2**. Not surprisingly, the co-ordination around the silicon tetrahedron carrying the phenyl substituent is distorted, exhibiting one aberrant tetrahedral angle in both structures, 107.95(11) and 107.76(24)°. This is attributed to both the influence of molecular packing and steric interactions between cage and substituent atoms: the shortest $\text{O}_{\text{cage}} \cdots \text{H}_{\text{phenyl}}$ distances are 2.682(4) and 2.811(5) Å respectively. Intermolecular contacts of the type $\text{O} \cdots \text{Si}$ often seen among the

Table 2 Selected bond lengths (Å) and angles (°) for compound **2**

Si(1)–C(1)	1.844(2)	Si(6)–O(15)	1.593(3)
Si(1)–O(10)	1.598(3)	Si(6)–O(11)	1.604(3)
Si(1)–O(1)	1.616(3)	Si(6)–O(1)	1.620(3)
Si(1)–O(6)	1.617(4)	Si(7)–O(11)	1.591(3)
Si(2)–O(6)	1.571(4)	Si(7)–O(12)	1.602(3)
Si(2)–O(7)	1.583(3)	Si(7)–O(2)	1.613(3)
Si(2)–O(2)	1.607(3)	Si(8)–O(12)	1.598(3)
Si(3)–O(8)	1.592(4)	Si(8)–O(13)	1.601(4)
Si(3)–O(7)	1.602(3)	Si(8)–O(3)	1.605(3)
Si(3)–O(3)	1.613(3)	Si(9)–O(14)	1.602(4)
Si(4)–O(4)	1.601(3)	Si(9)–O(13)	1.606(4)
Si(4)–O(8)	1.609(4)	Si(9)–O(4)	1.618(3)
Si(4)–O(9)	1.612(4)	Si(10)–O(14)	1.594(4)
Si(5)–O(10)	1.583(4)	Si(10)–O(15)	1.601(3)
Si(5)–O(9)	1.589(4)	Si(10)–O(5)	1.611(3)
Si(5)–O(5)	1.620(3)		
O(10)–Si(1)–O(1)	109.4(2)	O(12)–Si(8)–O(13)	109.5(2)
O(10)–Si(1)–O(6)	107.8(2)	O(12)–Si(8)–O(3)	110.4(2)
O(1)–Si(1)–O(6)	109.7(2)	O(13)–Si(8)–O(3)	109.8(2)
O(10)–Si(1)–C(1)	110.5(2)	O(14)–Si(9)–O(13)	109.5(2)
O(1)–Si(1)–C(1)	111.54(14)	O(14)–Si(9)–O(4)	110.2(2)
O(6)–Si(1)–C(1)	107.9(2)	O(13)–Si(9)–O(4)	109.6(2)
O(6)–Si(2)–O(7)	109.9(2)	O(14)–Si(10)–O(15)	109.6(2)
O(6)–Si(2)–O(2)	109.6(2)	O(14)–Si(10)–O(5)	109.8(2)
O(7)–Si(2)–O(2)	110.6(2)	O(15)–Si(10)–O(5)	109.8(2)
O(8)–Si(3)–O(7)	109.0(2)	Si(1)–O(1)–Si(6)	145.2(2)
O(8)–Si(3)–O(3)	110.1(2)	Si(2)–O(2)–Si(7)	149.1(2)
O(7)–Si(3)–O(3)	110.1(2)	Si(8)–O(3)–Si(3)	150.9(2)
O(4)–Si(4)–O(8)	110.3(2)	Si(4)–O(4)–Si(9)	150.8(2)
O(4)–Si(4)–O(9)	110.2(2)	Si(10)–O(5)–Si(5)	145.3(2)
O(8)–Si(4)–O(9)	110.0(2)	Si(2)–O(6)–Si(1)	155.6(2)
O(10)–Si(5)–O(9)	108.3(2)	Si(2)–O(7)–Si(3)	154.7(2)
O(10)–Si(5)–O(5)	110.0(2)	Si(3)–O(8)–Si(4)	154.5(3)
O(9)–Si(5)–O(5)	111.1(2)	Si(5)–O(9)–Si(4)	150.6(2)
O(15)–Si(6)–O(11)	109.6(2)	Si(5)–O(10)–Si(1)	162.7(3)
O(15)–Si(6)–O(1)	110.3(2)	Si(7)–O(11)–Si(6)	155.6(2)
O(11)–Si(6)–O(1)	110.2(2)	Si(8)–O(12)–Si(7)	156.3(2)
O(11)–Si(7)–O(12)	109.9(2)	Si(8)–O(13)–Si(9)	150.5(2)
O(11)–Si(7)–O(2)	109.7(2)	Si(10)–O(14)–Si(9)	157.4(2)
O(12)–Si(7)–O(2)	110.2(2)	Si(6)–O(15)–Si(10)	157.4(2)

hydrospherosiloxanes are scarce in **1** and **2**. Only in the packing of **2** there are contacts less than the commonly used threshold of 3.7 Å, the shortest being 3.652(3) Å.

Vibration structure

Molecules **1** and **2** consist of 38 and 45 atoms, respectively. We expect therefore 108 fundamental vibrations for **1** and 129 for **2**, which are, referred to the overall symmetry C_1 , all active. In spite of this high number an assignment of the vibrations is possible if the spectrum is considered as being built up from those of the independent vibrating moieties. This approach is especially suited for organosilicon compounds because of the vibrational insulation provided by the silicon atom. This insulating effect can probably be attributed in part to the greater size and mass of silicon compared to carbon.¹⁶ We have shown that the IR spectrum of hexylhepta-hydrooctasilasesquioxane ($C_6H_{13}H_7Si_8O_{12}$) can be interpreted by correlating it with those of the three molecules $H_8Si_8O_{12}$, $Si[C_6H_{13}(OSiMe_3)_3]$, and $SiH(OSiMe_3)_3$.⁷ However, a more detailed analysis is desirable because empirical assignments of this kind are not fully reliable and do not give insight into mechanisms such as ring-opening vibrations or shifts of the Si–C modes. For $RH_7Si_8O_{12}$ ($R = CH_2CH_2Ph$ or $CH=CHPh$) we performed a normal coordinate analysis of all fundamentals, which provided the additional information necessary for an unambiguous assignment.⁸ Comparison of the IR and Raman spectra of **1** and **2** shows that the vibrational spectra of the two molecules are very similar. Many lines of **2** are, however, broader than those of **1** and especially the

Raman-active ring-opening vibrations are suitable for distinguishing the two molecules (Fig. 2).

To divide the spectra into the features of the independent vibrating moieties we used spectral correlations as well as a normal coordinate analysis. The spectrum of the phenyl substituent was compared with those of different phenylsilanes,^{17–21} and the siloxane cages of **1** and **2** were correlated with $H_8Si_8O_{12}$ ²² and $H_{10}Si_{10}O_{15}$,⁹ respectively. Figs. 3 and 4 show the division of the IR and the Raman spectra of **1** into the lines of the siloxane cage $H_7Si_8O_{12}$, the phenyl substituent and the connecting moiety $O_3Si-C(CH_3)_2$. In Table 3 the results of the normal mode calculation for **1** are compared with the measured frequencies. It illustrates that all fundamentals can be assigned and interpreted in terms of group frequencies. The symmetries refer to the local symmetry of the siloxane cage (C_{3v}) and the phenyl ring (C_{2v}), respectively. The vibrations of the siloxane cage are also correlated with those of the $O_4H_8Si_8O_{12}$ molecule. The classification of the vibrations is based on the potential-energy distribution of each normal mode in terms of internal coordinates as proposed by Morino and Kuchitsu.²³ The phenyl group is also classified according to Whiffen's notation.²⁴ Force constants describing the Si–C bond were determined and are listed in Table 4. The same analysis, with identical force constants, was carried out for **2** and the results obtained are similar and therefore not tabulated.

Vibrations of the phenyl group. The vibrational spectra of phenylsilanes are well understood and for several a consistent assignment of all frequencies was achieved with the help of spectral correlations¹⁸ and model calculations.²⁰ A common procedure to classify their vibrations is to consider the substituent of the phenyl ring as a point mass, which leads to a local symmetry of C_{2v} . Under this assumption 21 in-plane ($11 A_1$, $10 B_1$) and nine out-of-plane ($3 A_2$, $6 B_2$) fundamentals result. Whiffen refers to these vibrations using the letters of the alphabet.²⁴ He describes their form schematically as C–H stretch (z_1-z_5), C–H in-plane bending ($a-e$), C–H out-of-plane bending ($f-j$), C–C stretch ($k-o$), in-plane ring deformation ($p-t$) and out-of-plane ring deformation ($v-y$). Only six of these 30 vibrations are influenced by the substituent of the phenyl ring. These X-sensitive vibrations are denoted q (A_1), r (A_1), t (A_1), u (B_1), x (B_2) and y (B_2).

The normal coordinate analysis of compounds **1** and **2** is in general agreement with the characterization of the fundamentals of monosubstituted halogenobenzenes by Whiffen.²⁴ In the potential energy analysis, however, the vibrations m , n , e and d all show similar contributions of C–C stretching and C–H bending movement. We base the assignment to a type of vibration on the greatest contribution to the potential energy, and in Table 3 therefore characterize m and n as C–H bending, and e and d as C–C stretching vibrations. This is in contrast to the characterization by Whiffen, based on empirical group frequencies and symmetry considerations, where m and n appear as stretching and d and e as bending motions.

The six vibrations known to be influenced by the substituent appear at almost the same wavenumbers in the spectra of compounds **1** and **2** and we therefore discuss them in detail only for **1**. The potential energy analysis shows that these vibrations are delocalized over the inorganic and the organic part. Three of them (q , r and t) involve appreciable Si–C stretching, in accordance with the findings of Whiffen for halogenobenzenes. The vibration q could not be found in the IR and Raman spectra of **1**. It was calculated at 1105 cm^{-1} , close to the value for phenylsilane¹⁹ and chlorophenylsilane.¹⁷ The highest Si–C stretching character (30%) is possessed by r and it can be regarded as the Si–C stretching vibration. It is assigned to the sharp band at 730 cm^{-1} in the IR and Raman spectra, see Figs. 3 and 4. The mode t is expected in the range $250\text{--}550\text{ cm}^{-1}$ and is known to be partly dependent on the mass of the substituent.¹⁸ We assign it to the peak at 240 cm^{-1} in the Raman spectrum,

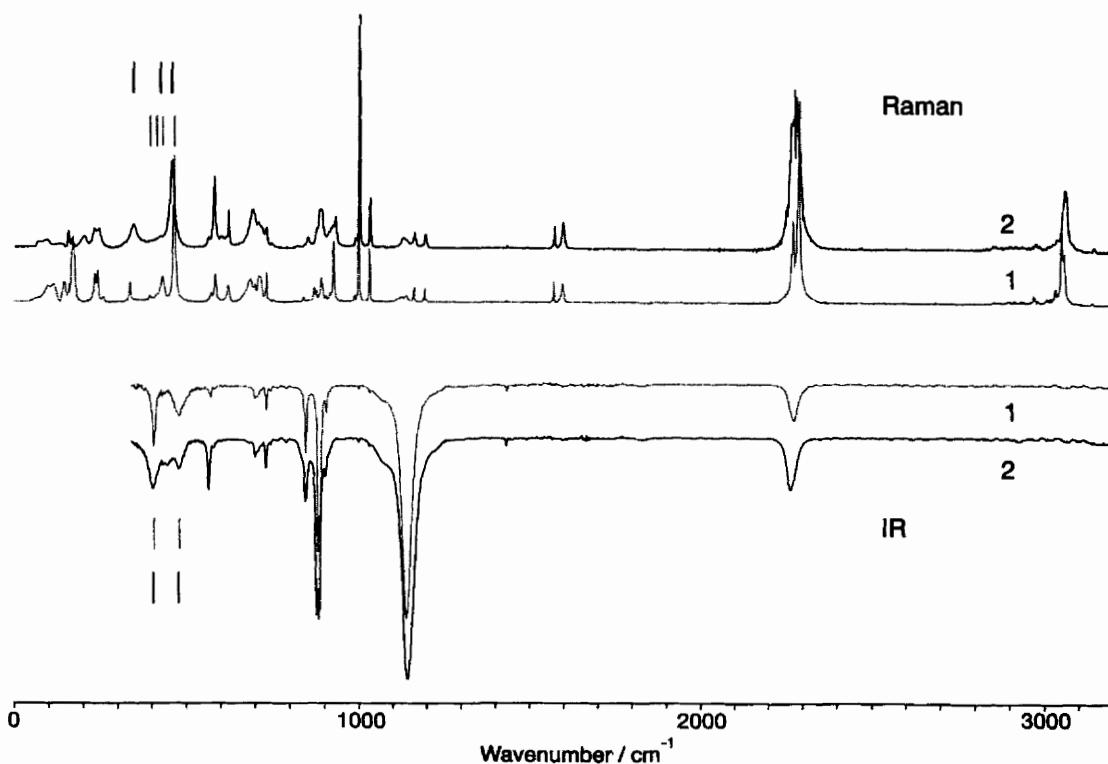


Fig. 2 Comparison of the Fourier-transform Raman spectra (top) and the IR transmission spectra (bottom) of compounds **1** (dotted line) and **2** (solid line). The ring-opening vibrations are marked with vertical dotted lines for **1** and with solid lines for **2**

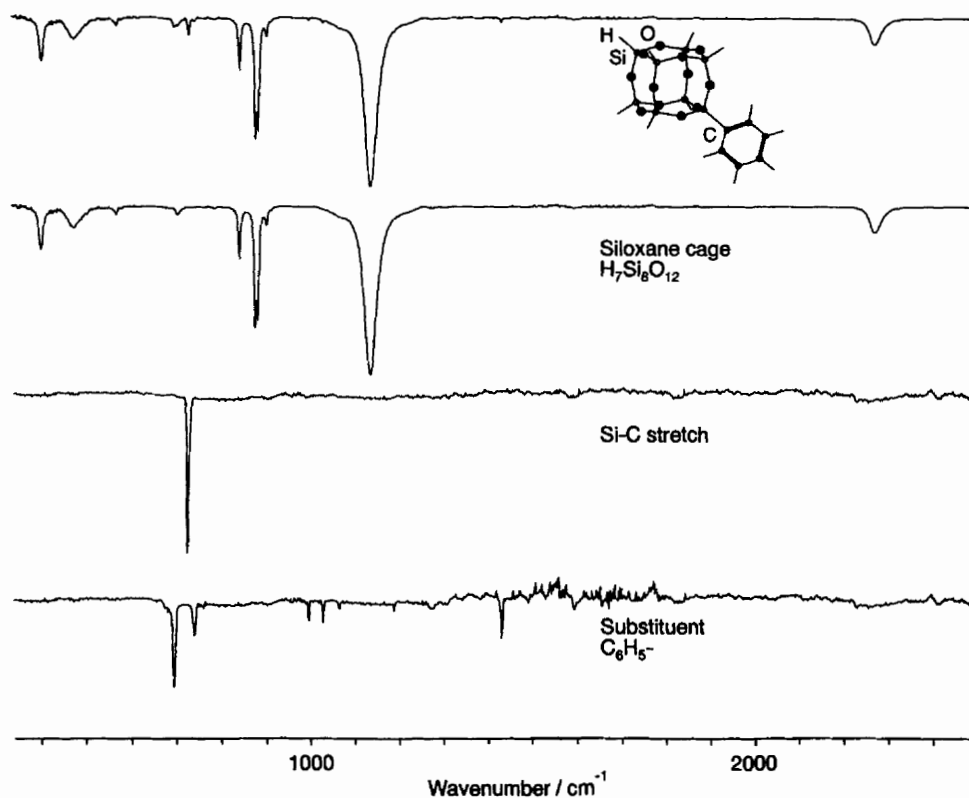


Fig. 3 Infrared transmission spectrum of compound **1** divided into the lines due to the siloxane cage, the phenyl ring (ordinate expanded by a factor of ten), and the Si-C stretch (ordinate expanded by a factor of ten)

which falls a little below the expected range. It was calculated at 236 cm^{-1} and bears 20% Si-C stretching character. The shift to lower energy is probably caused by the large mass of the spherosiloxane cage. The mode *u* can be looked upon as the in-plane ring rotation against the substituent, in our case the cage, and falls between 170 and 410 cm^{-1} . It was measured at 257 cm^{-1} in the Raman spectrum and calculated at 259 cm^{-1} . This

motion is strongly dominated by the Si-C-C bending coordinate (52%) and also has 17% $\delta(\text{O-Si-C})$ character. The vibrations *x* and *y* are both out-of-plane bending motions: *y* falls between 420 and 530 cm^{-1} and should be strong in the IR and absent or weak in the Raman spectrum, it was calculated at 471 cm^{-1} and therefore coincides with the siloxane cage vibration at 475 cm^{-1} . Vibration *x* is expected between 150 and

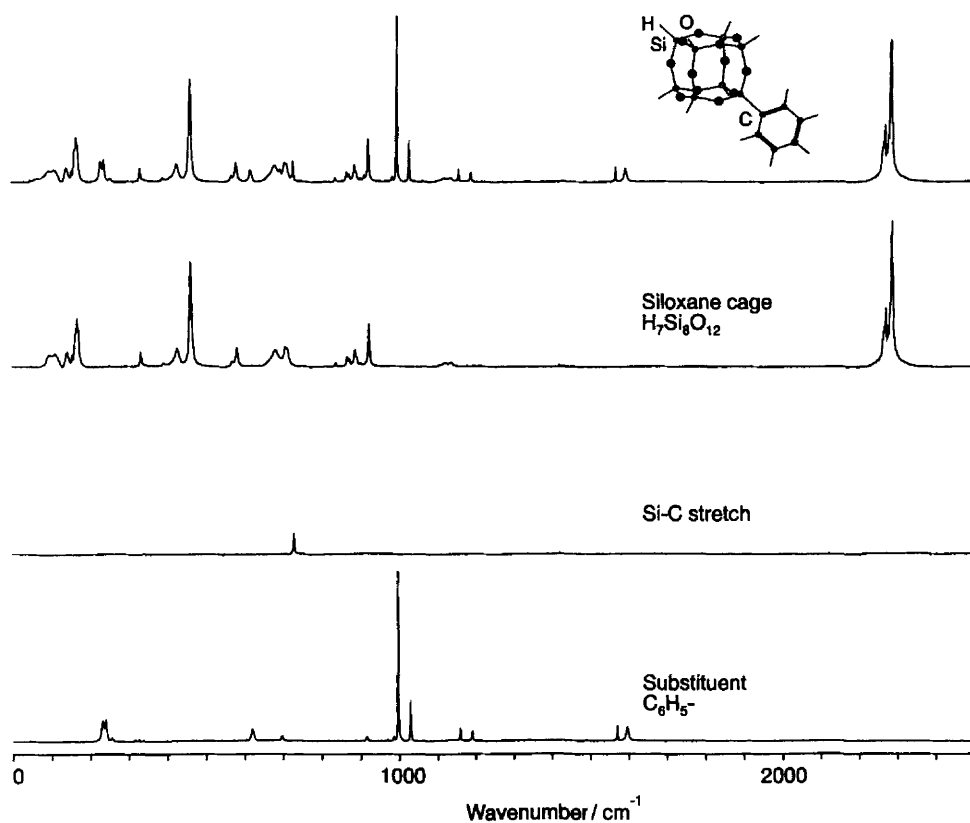


Fig. 4 Fourier-transform Raman spectrum of compound 1 divided into the lines due to the siloxane cage, the phenyl ring, and the Si-C stretch

280 cm^{-1} . We assign it to the band at 232 cm^{-1} in the Raman spectrum. It is calculated at 223 cm^{-1} and has substantial O-Si-C bending character (29%). All other vibrations of the phenyl ring show within a few wavenumbers the same frequencies as those for phenylsilane and chlorophenylsilane.

In the IR and Raman spectra of compound 2 vibrations ν (IR: 729, Raman 730), τ (Raman 243) and χ (Raman 230 cm^{-1}) could be detected. The mode μ is calculated at 261 cm^{-1} for 2 and is probably obscured by the broad peak due to τ .

Vibrations of the siloxane cage. The IR and the Raman spectra of $\text{H}_8\text{Si}_8\text{O}_{12}$ consist of 6 (6 T_{1u}) and 13 (3 A_{1g} , 4 E_g , 6 T_{2g}) active fundamentals, respectively. For $\text{H}_{10}\text{Si}_{10}\text{O}_{15}$ these numbers increase to 16 IR-active (6 A''_2 , 10 E''_1) and 27 Raman-active (7 A'_1 , 11 E'_2 , 9 E'_1) fundamentals. The spectra of both molecules were analysed in detail recently.^{9,10,22} The introduction of a substituent influences the vibrations of the siloxane cage by (i) changing the structure of the Si_8O_{12} and $\text{Si}_{10}\text{O}_{15}$ framework, respectively, (ii) reducing the symmetry when replacing an H by a C atom, and (iii) vibrational coupling with modes of the connecting moiety $\text{O}_3\text{Si}-\text{C}(\text{CH})_2$ or of the phenyl ring. Point (i) is manifested in the crystal structure where a distortion of the silicon tetrahedron carrying the phenyl substituent is observed. This distortion is found to have little influence on the vibrational spectra and is thus, in reality, expected to be negligible. It may cause splitting of some degenerate bands of $\text{O}_h\text{-H}_8\text{Si}_8\text{O}_{12}$ and $D_{5h}\text{-H}_{10}\text{Si}_{10}\text{O}_{15}$ but is not expected to be sufficient to allow forbidden bands to gain significant intensity. The analysis showed that the symmetry reduction (ii) is best described by treating the substituent as a point mass, with new force constants, leading to local C_{3v} and C_s symmetry for compounds 1 and 2, respectively. Most splittings and new bands of the siloxane cage can be understood assuming these local symmetries. Their importance is manifested in the strong resemblance of the vibrational spectra of different monosubstituted octasilasesquioxanes. Point (iii) is important in the cases where peaks or splittings cannot be

explained by the influence of a point mass. The potential energy distribution shows that in these cases the vibrations involve coordinates of the connecting moiety $\text{O}_3\text{Si}-\text{C}(\text{CH})_2$ or of the phenyl ring and the concept of local symmetries no longer applies.

Assuming C_{3v} and C_s cage symmetry, respectively, we expect for the Si_8O_{12} cage 19 A_1 and 26 E vibrations, both IR and Raman active, and 7 inactive A_2 vibrations. For the $\text{Si}_{10}\text{O}_{15}$ cage all degeneracies are removed which leads to 53 A' and 46 A'' vibrations, both IR and Raman active. Comparison of the IR and Raman spectra of compounds 1 and 2 with those of the corresponding unsubstituted siloxane cages shows striking similarities indicating a much simpler behaviour, however. This corresponds with the analysis of $(\text{C}_6\text{H}_{13})\text{H}_7\text{Si}_8\text{O}_{12}$,⁷ which shows that the symmetry reduction induced by the substituent leads only to small band splittings and that the spectra are still dominated by bands active for the unsubstituted compounds. It is therefore useful to refer to the symmetries of $\text{O}_h\text{-H}_8\text{Si}_8\text{O}_{12}$, as we have done in Table 3, and of $D_{5h}\text{-H}_{10}\text{Si}_{10}\text{O}_{15}$ to analyse the spectra of the substituted compounds.

The IR spectrum of compound 1 is similar to that measured for $(\text{C}_6\text{H}_{13})\text{H}_7\text{Si}_8\text{O}_{12}$ due to the weak intensities of the vibrations of the organic substituents in comparison with the siloxane cage motions. In Fig. 3 the IR spectrum of 1 is shown as a whole (top) and divided into the bands of the siloxane cage, the Si-C stretch and the phenyl group. The last two are enlarged by a factor of ten. Most of the bands that dominate the whole spectrum can be correlated with the IR-active T_{1u} bands of $\text{H}_8\text{Si}_8\text{O}_{12}$. Only a few bands could be detected that correlate with inactive vibrations of $\text{H}_8\text{Si}_8\text{O}_{12}$. Three, at 915, 905 and 844 cm^{-1} are O-Si-H bendings. Their origins are the symmetry-forbidden E_g , T_{2u} and T_{1g} modes of the $\text{O}_h\text{-H}_8\text{Si}_8\text{O}_{12}$ molecule. The two bands at 718 and 704 cm^{-1} correlate with an IR-inactive E_g mode of $\text{H}_8\text{Si}_8\text{O}_{12}$. They are also observed in the Raman spectrum of 1.

In the Raman spectrum of compound 1 peak intensities pertaining to the siloxane cage and to the substituent are of the

Table 3 Observed and calculated frequencies for compound **1** and their assignment (ν = stretch, δ = bending, γ = out-of-plane bending, τ = torsion; a,b...z₅, Whiffen's notation, X-sens. = substituent-sensitive vibrations, r.o.v. = ring-opening vibration)

Symmetry type		Wavenumber/cm ⁻¹			Vibration type
<i>O_h</i>	<i>C_{3v}/C_{2v}</i>	IR	Raman	Calc.	
			3141		2 × 1575
	B ₁	3075	3076	3062	ν (C-H), z ₄
	A ₁	3061	3060	3054	ν (C-H), z ₁
	A ₁		3052	3049	ν (C-H), z ₂
	B ₁		3034	3041	ν (C-H), z ₅
	A ₁		3021	3038	ν (C-H), z ₃
			3010		1432 + 1591
			2986		1432 + 1575
			2972		2 × 1497
A _{1g}	A ₁		2291	2275	ν (Si-H)
T _{2g}	E, A ₁		2285, 2278	2275	ν (Si-H)
T _{1u}	E, A ₁	2274	2275, 2269	2275	ν (Si-H)
	A ₁	1596	1595	1591	ν (C-C), k
	B ₁		1570	1575	ν (C-C), l
	A ₁	1492	1490	1497	δ (C-H), m
	B ₁	1432	1431	1432	δ (C-H), n
	B ₁			1336	ν (C-C), o
	B ₁			1279	ν (C-C), e
	A ₁	1191	1192	1186	δ (C-H), a
T _{1g}	A ₂ , E			1161, 1162/1160	ν_{asym} (Si-O-Si)
E _u	E			1159/1157	ν_{asym} (Si-O-Si)
	B ₁		1160	1155	δ (C-H), c
T _{1u}	A ₁ , E	1140, 1140		1157, 1142/1141	ν_{asym} (Si-O-Si)
T _{2g}	A ₁ , E		1140, 1121	1132, 1115	ν_{asym} (Si-O-Si)
	A ₁			1105	X-sens., q
A _{2u}	A ₁			1083	ν_{asym} (Si-O-Si)
	B ₁	1069	1068	1061	ν (C-C), d
	A ₁	1031	1030	1032	δ (C-H), b
	A ₁	999	999	1004	Ring, p
	B ₂		987	981	γ (C-H), j
	A ₂			966	γ (C-H), h
E _g	E	915	925	921	δ (O-Si-H)
T _{2u}	A ₂ , E	—, 905	—, 904	918, 910/908	δ (O-Si-H)
	B ₂		915	911	γ (C-H), i
T _{2g}	A ₁ , E	—, 886	893, 889	894, 889	δ (O-Si-H)
T _{1u}	A ₁ , E	886, 881	875, 868	882, 874	δ (O-Si-H)
T _{1g}	A ₂ , E	—, 844	—, 839	865, 864	δ (O-Si-H)
	A ₂			849	γ (C-H), g
	B ₂	743		747	γ (C-H), f
A _{2u}	A ₁	730	730	731	X-sens.; ν (Si-C), r
E _g	E	718/704	712/707	711/705	ν_{sym} (Si-O-Si)
	B ₂	697	696	702	γ (C-C), v
T _{2u}	E, A ₂		682, 682	687, 683	ν_{sym} (Si-O-Si)
T _{2g}	E, A ₁			625/621, 615	ν_{sym} (Si-O-Si)
	B ₁		618	614	δ (C-C), s
T _{1u}	A ₁ , E	—, 569	—, 569	591, 573	ν_{sym} (O-Si-O)
A _{1g}	A ₁		580	574	δ (O-Si-O)
T _{1u}	E, A ₁	475, 475		500/491, 478	ν_{sym} (O-Si-O), r.o.v.
	B ₂	475		471	X-sens., y
A _{1g}	A ₁		462	467	ν_{sym} (O-Si-O), r.o.v.
T _{2g}	A ₁ , E		427	430, 428/425	δ (O-Si-O), r.o.v.
E _g	E		412	422	δ (O-Si-O), r.o.v.
	A ₂			405	γ (C-C), w
T _{1u}	A ₁ , E	402, 402	392	403, 399	δ (O-Si-O), r.o.v.
T _{1g}	E, A ₂			364/361, 356	δ (O-Si-O)
A _{2u}	A ₁		333	329	δ (O-Si-O)
T _{2u}	E, A ₁			306/305, 303	δ (O-Si-O)
	B ₁		257	259	X-sens., u
	A ₁		240	236	X-sens., t
	B ₂		232	223	X-sens., x
T _{2g}	E, A ₂		172/169, 143	170/168, 137	δ (O-Si-O)
E _u	E		165/157	158/155	δ (O-Si-O)
E _g	E		112/97	106/100	δ (Si-O-Si)
T _{2u}	E, A ₂			75, 71	δ (Si-O-Si)
E _u	E			39	δ (O-Si-C)
				27	τ (O ₃ Si-CC ₂)
A _{2g}	A ₂			16	τ (Si-O-Si)

same order of magnitude, as can be seen in Fig. 4. The most dominant peaks of the siloxane cage spectrum correlate with Raman-active modes of H₈Si₈O₁₂ (A_{1g}, E_g, T_{2g}). Treating the substituent as a point mass we expect for the T_{2g} modes a

splitting into A₁ and E, whereas the doubly degenerate modes should appear as single lines. Three out of the six T_{2g} modes indeed show splittings into doublets, namely the ν (Si-H), ν_{asym} (Si-O-Si) and δ (O-Si-H). For the δ (O-Si-O), at 171 cm⁻¹

Table 4 Force constants obtained from the normal coordinate analysis of compound **1**

Force constant*	Value
$F(\nu\text{SiC})$	3.389
$F(\delta\text{SiCC})$	0.591
$F(\tau\text{SiC})$	0.03
$F(\gamma\text{SiC})$	0.329
$F(\delta\text{OSiC})$	0.804
$F(\nu\text{CC}, \nu\text{SiC})$	0.081
$F(\delta\text{CCC}, \delta\text{SiCC})$	0.218
$F(\nu\text{SiO}, \delta\text{OSiC})$	0.551

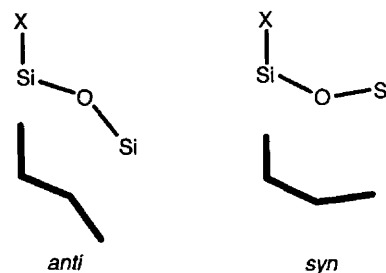
* Units: stretching constants (ν), $\text{mdyn } \text{\AA}^{-1}$; bending and torsional constants (δ, γ, τ), $\text{mdyn } \text{\AA} \text{ rad}^{-2}$; stretch-bend interactions (ν, δ), $\text{mdyn } \text{rad}^{-1}$; $\text{dyn} = 10^{-5} \text{ N}$.

for $\text{H}_8\text{Si}_8\text{O}_{12}$, a strong splitting into an E and an A_1 (143 cm^{-1}) is observed, in accordance with the symmetry reduction from O_h to C_{3v} . The additional splitting of the E mode (172 and 169 cm^{-1}) can only be understood assuming a symmetry lower than C_{3v} . The same is true for two of the four E_g modes, which appear as doublets, namely $\nu_{\text{sym}}(\text{Si-O-Si})$ at 712 and 707 cm^{-1} and $\delta(\text{Si-O-Si})$ at 112 and 97 cm^{-1} . The reason for the splitting of these doubly degenerate modes is vibrational coupling with modes of the connecting moiety $\text{O}_3\text{Si-C}(\text{CH}_2)_2$. In addition to the lines correlating with Raman-active vibrations of $\text{H}_8\text{Si}_8\text{O}_{12}$, several peaks are found that correspond with vibrations inactive in $\text{H}_8\text{Si}_8\text{O}_{12}$. The Si-H stretching and the O-Si-H bending regions can both fully be understood assuming C_{3v} symmetry for the cage, indicating that these vibrations are purely located on the siloxane part.

The correlation of the IR spectrum of compound **2** with that of $\text{H}_{10}\text{Si}_{10}\text{O}_{15}$ shows a broadening of bands due to splittings and bands that become active under the symmetry reduction. Between 840 and 950 cm^{-1} additional absorptions occur that are assigned to O-Si-H bendings. The striking resemblance of the IR spectra of **1** and **2** (Fig. 2) is due to the close similarity observed for the IR spectra of $\text{H}_8\text{Si}_8\text{O}_{12}$ and $\text{H}_{10}\text{Si}_{10}\text{O}_{15}$ ⁹ and to the similar interaction of the Si_8O_{12} and $\text{Si}_{10}\text{O}_{15}$ siloxane cages with the substituent. The most obvious difference occurs in the $\nu_{\text{sym}}(\text{O-Si-O})$ region: $\nu_{\text{sym}}(\text{O-Si-O})$ of $\text{PhH}_9\text{Si}_{10}\text{O}_{15}$ at 563 cm^{-1} is stronger than the corresponding vibration of $\text{PhH}_7\text{Si}_8\text{O}_{12}$ at 569 cm^{-1} .

In the Raman spectrum of compound **2** no splittings are observed except for the Si-H stretching and O-Si-H bending region, where the spectrum becomes rather complicated. The high number of frequencies expected assuming C_s symmetry for the cage and the broad peaks in this region make some assignments difficult, but all main features are well understood. The resemblance between the Raman spectra of **1** and **2** is again striking. Differences are observed in the pattern of the O-Si-H bending and Si-H stretching vibrations. A clear distinction is possible in the ring-opening region, where the five-membered-ring opening vibration gives rise to a peak of medium intensity at 344 cm^{-1} in the Raman spectrum of $\text{PhH}_9\text{Si}_{10}\text{O}_{15}$.

Si-C stretch and O-Si-C bending. The substitution of one hydrogen atom by a phenyl group turns a Si-H stretch into a Si-C stretch and two O-Si-H bendings into two O-Si-C bendings. These are the only vibrations that show a large shift when we correlate the unsubstituted with the substituted molecules. We have found that the force constants in Table 4 are valid for both compounds **1** and **2**. The Si-C stretch is assigned in **1** and **2** to the vibration at 730 cm^{-1} , *i.e.* at higher wavenumber than for phenylsilane (692 cm^{-1}) and chlorophenylsilane (717 cm^{-1}); $\nu(\text{Si-C})$ is known to be at higher wavenumber for siloxanes and chorosilanes than for silanes.^{25,26} For spherosiloxanes we expect an additional rise in frequency compared to other siloxanes, caused by the C-Si-O-Si conformation. The



Scheme 2 The *anti* and *syn* conformations of cage and open siloxanes

cage structure of the spherosiloxanes allows only an *anti* C-Si-O-Si conformation as shown on the left-hand side of Scheme 2, which was found to show a higher Si-C bond order than the *syn* conformation realized in the open structure.²⁷

The compounds $\text{RH}_7\text{Si}_8\text{O}_{12}$ ($\text{R} = \text{CH}_2\text{CH}_2\text{Ph}$, $\text{CH}=\text{CHPh}$ or Ph) exemplify Si-C_{alkyl}, Si-C_{vinyl} and Si-C_{phenyl} bonds, respectively. The corresponding stretching frequencies, force constants and bond lengths are in Table 5. In all three cases the potential-energy distribution indicates a coupling of the Si-C stretch with the C-C stretching and C-C bending motions of the phenyl group and the Si-O stretch of the siloxane cage. The off-diagonal elements in Table 4 are therefore to be considered important. In $\text{RH}_7\text{Si}_8\text{O}_{12}$ ($\text{R} = \text{CH}_2\text{CH}_2\text{Ph}$ or $\text{CH}=\text{CHPh}$) we observe in addition a coupling with the C-C_{phenyl} stretching motion: $\nu(\text{Si-C}_{\text{phenyl}})$ has 30% Si-C stretching character, $\nu(\text{Si-C}_{\text{alkyl}})$ 39% and $\nu(\text{Si-C}_{\text{vinyl}})$ 49%. A comparison of the Si-C stretching force constants shows a higher value for Si-C_{vinyl} and Si-C_{phenyl} than Si-C_{alkyl}. This indicates that the Si-C bond is stronger in $\text{RH}_7\text{Si}_8\text{O}_{12}$ ($\text{R} = \text{Ph}$ or $\text{CH}=\text{CHPh}$) compared to that in $(\text{PhCH}_2\text{CH}_2)_7\text{Si}_8\text{O}_{12}$. The low frequency of $\text{PhH}_7\text{Si}_8\text{O}_{12}$ is not due to the bond strength but probably caused by vibrational coupling or a mass effect, caused by the direct connection of the phenyl ring to the siloxane cage. This leads to a larger effective mass of the C atom in Si-C_{phenyl} than in Si-C_{vinyl} and Si-C_{alkyl}.

The O-Si-C bending motion cannot be assigned to one frequency only. The potential-energy analysis shows several frequencies below 260 cm^{-1} with O-Si-C bending character. In the Raman spectrum of compound **1** these are the vibrations at 257 (17%), 232 (29%), 112 (24%) and 97 cm^{-1} (14%). The E-type vibration calculated at 39 cm^{-1} with 30% O-Si-C bending character is below the experimental detection limit.

Ring-opening vibrations. The ring-opening vibrations are defined as normal modes in which all Si-O stretching and/or O-Si-O bending displacements of the considered ring are in phase. Detailed analysis of the vibrational spectra of $O_h\text{-H}_8\text{Si}_8\text{O}_{12}$ and $D_{5h}\text{-H}_{10}\text{Si}_{10}\text{O}_{15}$ showed that the energy region for the four-membered-ring opening vibrations is $490\text{--}390 \text{ cm}^{-1}$ and for the five-membered ring $440\text{--}250 \text{ cm}^{-1}$.⁹ Please note that the four- and five-membered rings are in fact built of four and five Si atoms plus four and five O atoms, respectively. Monosubstitution of the hydrosilasesquioxanes leads to a symmetry reduction raising the question if and to what extent the notion of the ring-opening vibrations remains applicable. When we treat the substituent as a point mass C_{3v} symmetry results for $\text{RH}_7\text{Si}_8\text{O}_{12}$. In this point group the only symmetry element relative to the four-membered ring is a mirror plane through two opposite silicon atoms of a ring, which leads to two sets of equivalent coordinates for the Si-O stretching and the O-Si-O bending displacements. The six four-membered rings form two sets of equivalent rings, illustrated in Scheme 3, one consisting of the three rings connected with the substituent (I in Scheme 3), and another consisting of the remaining three rings (II). In the double five-membered-ring the two-rings form two sets (I and II) and the five four-membered-rings three sets (I-III) of equivalent rings.

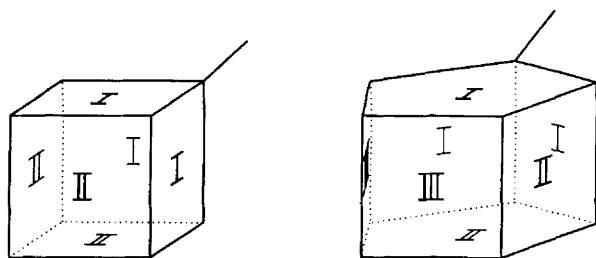
$\text{PhH}_7\text{Si}_8\text{O}_{12}$. Visual analysis of the vibrations using the

Table 5 Experimental Si–C stretching frequencies, bond distances, and force constants for different monosubstituted octasilasesquioxanes

Bond type	IR/cm ⁻¹	Raman/cm ⁻¹	<i>d</i> (Si–C)/Å	<i>F</i> (<i>v</i> SiC)/mdyn Å ⁻¹	Substituent
Si–C _{alkyl}	785	784	1.832	3.029	PhCH ₂ CH ₂
Si–C _{vinyl}	821	821			C ₆ H ₁₃
Si–C _{phenyl}	730	730	1.834	3.355	PhCH=CH Ph

Table 6 Calculated ring-opening vibrations (r.o.v.) of compound **1** correlated with vibrations/cm⁻¹ of H₈Si₈O₁₂

1		H ₈ Si ₈ O ₁₂	
A ₁	478	rings II	481 (T _{1u} , r.o.v.)
	467	rings I	446 (A _{1g} , r.o.v.)
	430	rings II	418 (T _{2g})
	403	rings I	397 (T _{1u} , r.o.v.)
E	500/491		481 (T _{1u} , r.o.v.)
	428/425		418 (T _{2g})
	422		423 (E _g , r.o.v.)
	399		397 (T _{1u} , r.o.v.)

**Scheme 3** Sets of equivalent rings in compounds **1** and **2**. The substituent is treated as a point mass

computer program MOBY²⁸ showed four A₁ and four E ring-opening vibrations, all occurring between 390 and 500 cm⁻¹. Table 6 shows that they all correlate with the ring-opening vibration of H₈Si₈O₁₂ with the exception of one A₁ and one E mode, which correlate with the T_{2g} mode of O_h-H₈Si₈O₁₂. It is interesting that in all 4 A₁ vibrations the ring-opening movement is predominantly located either on rings I or on II, as noted in Table 6. In the IR spectrum two ring-opening vibrations at 401 and at 475 cm⁻¹ can be detected. Compared to H₈Si₈O₁₂ they shift to higher wavenumbers by 2 and 10 cm⁻¹, respectively. The strongest peak in the Raman spectrum of H₈Si₈O₁₂ is the totally symmetric ring-opening⁹ mode at 456 cm⁻¹. For compound **1** this peak shows a small shift to 462 cm⁻¹ and a distinct decrease in intensity although it remains the strongest peak in this region. In contrast the vibration at 427 cm⁻¹, which correlates with the T_{2g} mode of H₈Si₈O₁₂ measured at 414 cm⁻¹, has gained intensity. This corresponds with the result of the normal coordinate analysis of **1** that shows a mixing of the two A₁ modes calculated at 467 and at 430 cm⁻¹. The mode at 430 cm⁻¹ has enhanced *v*_{sym}(O–Si–O) character and that at 467 cm⁻¹ enhanced *δ*(O–Si–O) character. For **1** both are ring-opening vibrations, whereas for H₈Si₈O₁₂ only the A_{1g} vibration at 456 cm⁻¹ is.

PhH₉Si₁₀O₁₅. Three vibrations with five-membered-ring opening character were found, all between 300 and 350 cm⁻¹. Two show a ring-opening movement for the ring I, which is connected with the substituent (calculated at 325 and 348 cm⁻¹) and one for ring II (334 cm⁻¹). The four-membered-ring openings are between 400 and 470 cm⁻¹. The vibration at 455 cm⁻¹ in the Raman spectrum is calculated at 453 cm⁻¹ and correlates with the ring-opening vibration of all four-membered-rings of H₁₀Si₁₀O₁₅ calculated at 450 cm⁻¹. It shows a decrease in intensity with the phenyl substitution and performs a ring opening only on rings II and III in

PhH₉Si₁₀O₁₅. No vibration was found where all four- or all five-membered-rings perform a ring-opening movement. We conclude that the notion of the ring-opening vibrations still makes sense with respect to the monosubstituted hydrospherosiloxanes and that these vibrations contribute in a significant and specific way to the low-frequency region.

Overtone and combination bands. Four of the ten absorptions in the IR spectrum of H₈Si₈O₁₂ are combination bands.²² These are less distinct for compound **1** and appear only as broad weak features. As they are barely resolved they were not included in Table 3. Most overtones and combination bands in the Raman spectrum of **1** occur in the C–H stretching region and were also found in the IR or Raman spectrum of chlorophenylsilane. They are overtones and combination bands of C–H bending or C–C stretching vibrations.¹⁷

Experimental

Physical methods

High-performance liquid chromatography was performed with a Merck-Hitachi LC 6200 pump, an Erma ERC 3511 solvent degasser, an Erma ERC 7512 refractive index detector and a Hewlett-Packard 3396A integrator. A 600 × 25 mm Polymer-Lab size-exclusion HPLC column (pore size 50 Å, particle size 10 μm) was used. Hexane (Romil Chemicals) was used as eluent. The flow rate was 6 cm³ min⁻¹ at room temperature. Proton, ¹³C and ²⁹Si NMR were recorded on a Bruker AC-300 instrument using CDCl₃ as solvent, mass spectra on a MAT-CH7A instrument. The elemental analyses were performed by the analytical department of Ciba-Geigy, Basel.

Spectroscopy

The IR transmission spectra were measured in CCl₄ with a BOMEM DA3.01 FTIR spectrometer equipped with a liquid-nitrogen cooled mercury cadmium telluride-detector (500–5000 cm⁻¹) and a DTGS detector (10–750 cm⁻¹). A KBr beam splitter was applied for measurements above 700 cm⁻¹, whereas in the range 350–700 cm⁻¹ a 3 μm Mylar beam splitter was used. The spectra were measured with a resolution of 1 cm⁻¹. Fourier-transform Raman spectra were recorded with the Bomem Raman accessory of the same spectrometer. The interferometer was equipped with a quartz beam splitter and a liquid-nitrogen-cooled InGaAs detector. The continuous-wave Nd³⁺-YAG laser (Quantronix Model 114) was run in the transverse electromagnetic mode TEM₀₀ at 9395 cm⁻¹. Rayleigh scattering was blocked by three holographic super notch filters (Kaiser Optical Systems) in 6° angle position. A 2 mm thick anodized aluminium plate with a 1 mm diameter hole into which the probe was slightly pressed, served as sample holder.

Normal coordinate analysis

The normal mode calculations were performed by the Wilson GF matrix method²⁹ using the computer program package QCMP 067.³⁰ The bond lengths and angles used for the siloxane cage were the same as for H₈Si₈O₁₂²² and H₁₀Si₁₀O₁₅.⁹ For the phenyl ring *d*(C–C) = 1.4 Å and *d*(C–H) = 1.084 Å were used and for the Si–C bond the value

Table 7 Experimental data for the crystal structure analysis of compounds **1** and **2***

Molecular formula	C ₆ H ₁₂ O ₁₂ Si ₈	C ₆ H ₁₄ O ₁₅ Si ₁₀
<i>M</i>	500.88	607.07
Crystal dimensions/mm	0.494 × 0.171 × 0.171	0.418 × 0.494 × 0.190
Crystal colour, shape	Colourless, transparent prism	Colourless, transparent plate
<i>a</i> /Å	7.409(2)	10.037(2)
<i>b</i> /Å	7.555(2)	10.734(2)
<i>c</i> /Å	18.250(3)	11.899(2)
α /°	81.29(1)	81.91(1)
β /°	80.00(1)	81.58(1)
γ /°	82.98(2)	74.33(1)
<i>U</i> /Å ³	989.5(4)	1214.1(3)
<i>D</i> _c /g cm ⁻³	1.681	1.661
μ (Mo-K α)/mm ⁻¹	0.596	0.604
Transmission factor range	0.8968–0.9153	0.7735–0.8650
<i>F</i> (000)	512	620
θ Range/°	2.29–27.52	1.74–28.01
<i>hkl</i> Ranges	–9 to 9, –9 to 9, 0–23	–13 to 13, –14 to 14, 0–15
No. unique data	4537	5859
No. observed data [$F_o^2 > 2\sigma(F_o^2)$]	2497	3402
Final <i>R</i> for unique data	0.0415	0.0623
Final <i>wR</i> for unique data	0.1170	0.1955
Goodness of fit, <i>S</i>	0.957	1.119
Final residuals, maximum and minimum/e Å ⁻³	0.31, –0.24	0.93, –0.89

* Details in common: triclinic, space group $P\bar{1}$; 291 K; *Z* = 2; ω –2 θ scans; largest and mean $\Delta/\sigma < 0.001$; $R = \sum||F_o| - |F_c||/\sum|F_o|$; conventional *R* based on $F_o > 4\sigma(F_o)$ observation criterion; $wR = [\sum w(F_o^2 - F_c^2)^2/\sum w(F_o^2)^2]^{1/2}$ where $w = 1/[\sigma^2(F_o^2) + (0.1225P)^2]$, for **1** and $1/[\sigma^2(F_o^2) + (0.0626P)^2]$ for **2**. $P = [\max(F_o^2, 0) + 2F_c^2]/3$; $S = [\sum w(F_o^2 - F_c^2)^2/(n - p)]^{1/2}$ where *n* is the number of observations and *p* the number of parameters.

determined by X-ray diffraction was taken [*d*(Si–C) = 1.835 Å]. The vibrational analysis of compounds **1** and **2** was performed using the modified general valence force field determined for H₈Si₈O₁₂ (Table 5 of ref. 22) to describe the inorganic part, and a modified valence force field for benzene for the organic part (Table 1 of ref. 31). Force constants involving the Si–C bond were introduced and their values determined by a fit to the IR and Raman data of **1**. For **2** the same force constant values were used as for **1**. The potential-energy distribution analysis was carried out as described in ref. 23.

Synthesis

Compounds **1** and **2** were prepared according to the method of Agaskar³² with the only exception that instead of 20 cm³ trichlorosilane 17.5 cm³ was used and in addition trichlorophenylsilane (5 cm³). The reaction mixture was filtered and the filtrate volume reduced to ca. 10 cm³ by evaporation. The crystals of H₈Si₈O₁₂ deposited were filtered off and the remaining yellow highly viscous solution injected on a size-exclusion HPLC column. The crude white product **1** was recrystallized from hexane–dichloromethane (1:1) as clear, colourless needles (250 mg, 0.13 mmol; 3.1%). Product **2** was recrystallized from the same solvent as colourless, square shaped flakes (40 mg, 0.02 mmol; 0.5%).

Compound **1** (Found: C, 14.6; H, 2.40; Si, 44.95. C₆H₁₂O₁₂Si₈ requires C, 14.4; H, 2.40; Si, 44.85%); IR 3075vw, 3061vw, 2274m, 1596vw, 1492vw, 1432w, 1215 (sh), 1191vw, 1140vs, 1069 (sh), 1031vw, 999vw, 915vw, 905w, 886s, 881s, 844m, 743vw, 730w, 718vw, 704w, 697w, 569w, 475m (br) and 402m cm⁻¹; NMR (CDCl₃, standard SiMe₄), ¹H (300 MHz), δ 4.30 (s, 3 H), 4.32 (s, 4 H), 7.3–7.7 (m, 3 H) and 7.5–7.7 (m, 2 H); ¹³C (75 MHz), δ 128.14 (2 C), 128.98 (SiC), 131.45 (1 C) and 134.19 (2 C); mass spectrum (70 eV, ca. 1.12×10^{-17} J) *m/z* 500 (100, [M]⁺), 453 (7), 423 (34) and 377 (14%). Compound **2**: IR: 3076vw, 2268m, 1598vw, 1432vw, 1220 (sh), 1191vw, 1146vs, 1080 (sh), 1031vw, 999vw, 920 (sh), 912vw, 902w, 885s, 878s, 847 (sh), 845m, 742vw, 730w, 705vw, 697w, 563m, 475m, 442w and 401m cm⁻¹; NMR (CDCl₃, standard SiMe₄), ¹H (300 MHz), δ 4.33 (s, 1 H), 4.32 (s, 2 H), 4.30 (s, 6 H), 7.3–7.7 (m, 3 H) and 7.5–7.7 (m, 2 H); ¹³C (75 MHz), δ 128.16 (2 C), 129.65 (SiC), 131.31

(1 C) and 134.04 (2 C); mass spectrum (70 eV) *m/z* 605 (100, M⁺), 559 (13), 528 (37), 483 (36), 437 (22) and 302 (15%, M²⁺).

Crystallography

The X-ray determinations are summarized in Table 7. Intensity data were collected on a STOE AED-2 four-circle instrument, using Mo-K α radiation (λ 0.710 73 Å) on samples sealed into quartz capillaries. Lattice parameters were derived from a least-squares fit of setting angles for 16 (compound **1**) and 20 (**2**) reflections in the ranges θ 14.43–19.42 (**1**) and 7.88–18.32° (**2**). Intensity variations were monitored using three reflections every 240 min with a maximum drop of 1.84 (**1**) and 1.41% (**2**), corrected by linear interpolation. Both structures were corrected for absorption by employing a Gaussian quadrature numerical method, final *R*_{int} factors being 0.0218 and 0.0161 respectively. The structures were solved by direct methods, SHELXS 86,³³ and refined on all $F^2 \geq 0$ with SHELXL 93,³⁴ applying anisotropic displacement factors to all non-hydrogen atoms. The Si–H distances were restrained to 1.461(5) Å, and C–H distances to 0.93 Å, the H-atom positions being geometrically idealized. In **1** the isotropic displacement of H(–Si) and H(–C) atoms were refined as two individual variables common to the chemically equivalent hydrogen atoms. In **2** the phenyl group exhibited substantial displacement, and was therefore treated as an idealized group with the hydrogens assigned 1.5 times the equivalent isotropic displacement factor of their pivotal carbon atoms. Molecular illustrations were made using SHELXTL PLUS.³⁵

Atomic coordinates, thermal parameters and bond lengths and angles have been deposited at the Cambridge Crystallographic Data Centre (CCDC). See Instructions for Authors, *J. Chem. Soc., Dalton Trans.*, 1996, Issue 1. Any request to the CCDC for this material should quote the full literature citation and the reference number 186/129.

Acknowledgements

This work was financed by the Schweizerischer Nationalfonds zur Förderung der wissenschaftlichen Forschung (project NF 20-040598.94/1) and by the Swedish Natural Science Research Council.

References

- 1 D. W. Scott, *J. Am. Chem. Soc.*, 1946, **68**, 356.
- 2 M. M. Sprung and F. O. Guenther, *J. Am. Chem. Soc.*, 1955, **77**, 3990, 3996.
- 3 A. J. Barry, W. H. Daudt, J. J. Domicone and J. W. Gilkey, *J. Am. Chem. Soc.*, 1955, **77**, 4248.
- 4 K. Olsson, *Ark. Kemi*, 1958, **13**, 367.
- 5 G. Calzaferri, *Proceedings, Tailor-made Silicon-Oxygen Compounds, from Molecules to Materials, Bielefeld*, eds. P. Jutzi and R. Corriu, 3–5th September 1995, pp. 149–169.
- 6 G. Calzaferri, R. Imhof and K. W. Törnroos, *J. Chem. Soc., Dalton Trans.*, 1993, 3741.
- 7 G. Calzaferri, R. Imhof and K. W. Törnroos, *J. Chem. Soc., Dalton Trans.*, 1994, 3123.
- 8 C. Marcolli, R. Imhof and G. Calzaferri, *Mikrochim. Acta*, 1996, in the press.
- 9 P. Bornhauser and G. Calzaferri, *J. Phys. Chem.*, 1996, **100**, 2035.
- 10 C. Marcolli, P. Lainé, R. Bühler, G. Calzaferri and J. Tomkinson, unpublished work.
- 11 F. J. Feher, K. J. Weller and J. J. Schwab, *Organometallics*, 1995, **14**, 2009.
- 12 F. J. Feher and K. J. Weller, *Organometallics*, 1990, **9**, 2638.
- 13 T. P. E. Auf der Heyde, H.-B. Bürgi, H. Bürgy and K. W. Törnroos, *Chimia*, 1991, **45**, 38.
- 14 K. W. Törnroos, G. Calzaferri and R. Imhof, *Acta Crystallogr., Sect. C*, 1995, **51**, 1732.
- 15 H.-B. Bürgi, K. W. Törnroos, G. Calzaferri and H. Bürgy, *Inorg. Chem.*, 1993, **32**, 4914.
- 16 A. L. Smith, *Spectrochim. Acta*, 1960, **16**, 87.
- 17 A. L. Smith, *Spectrochim. Acta, Part A*, 1967, **23**, 1075.
- 18 A. L. Smith, *Spectrochim. Acta, Part A*, 1968, **24**, 695.
- 19 F. Höfler, *Monatsh. Chem.*, 1976, **107**, 411.
- 20 F. Höfler, *Monatsh. Chem.*, 1976, **107**, 705.
- 21 J. R. Durig, K. L. Hellams and J. H. Mulligan, *Spectrochim. Acta, Part A*, 1972, **28**, 1039.
- 22 M. Bärtsch, P. Bornhauser, G. Calzaferri and R. Imhof, *J. Phys. Chem.*, 1994, **98**, 2817.
- 23 Y. Morino and K. Kuchitsu, *J. Chem. Phys.*, 1952, **20**, 1809.
- 24 D. H. Whiffen, *J. Chem. Soc.*, 1956, 1350.
- 25 H. Kriegsmann, *Z. Anorg. Allg. Chem.*, 1959, **299**, 138.
- 26 H. Kriegsmann, *Ber. Bunsenges. Phys. Chem.*, 1961, **65**, 342.
- 27 M. Bärtsch, G. Calzaferri and C. Marcolli, *Res. Chem. Intermed.*, 1995, **21**, 577.
- 28 U. Höweler, MOBY, *Molecular Modelling on the PC*, Version 1.6F, Springer, Berlin, 1993.
- 29 E. B. Wilson, jun., J. C. Decius and P. C. Cross, *Molecular Vibrations*, McGraw-Hill Book Co., New York, 1955.
- 30 D. F. McIntosh and M. R. Peterson, QCMP 067, General Vibrational Analysis System, Quantum Chemistry Program, Bloomington, IN, Exchange, 1988.
- 31 R. W. Snyder and P. C. Painter, *Polymer*, 1981, **22**, 1629.
- 32 P. A. Agaskar, *Inorg. Chem.*, 1991, **30**, 2707.
- 33 G. M. Sheldrick, *Acta Crystallogr., Sect. A*, 1990, **46**, 467.
- 34 G. M. Sheldrick, SHELXL 93, University of Göttingen, 1993.
- 35 G. M. Sheldrick, SHELXTL PLUS, Release 4.1, Siemens Analytical X-ray Instruments., Madison, WI, 1990.

Received 28th February 1996; Paper 6/01419D